APPLICATION OF WAVELET TRANSFORM TO STEADY-STATE APPROXIMATION OF POWER ELECTRONICS WAVEFORMS

Ming Liu, Pik Wan Michelle Ho and Chi K. Tse

Dept. of Electronic & Information Engineering
The Hong Kong Polytechnic University
Kowloon, Hong Kong, China

Jie Wu

College of Electrical Engineering
South China University of Technology
Guangzhou, China

ABSTRACT

Waveforms arising from power electronics circuits often contain slowly changing segments with high-frequency details concentrated near the switching instants. Such a feature is consistent with the localization property of wavelets which are known in the signal processing literature to be highly suitable for describing fast changing edges embedded in slowly varying backgrounds. This paper considers the application of wavelet approximation to the steady-state analysis of power electronics circuits. A procedure that involves mixing wavelets of different levels is described. When applied to power electronics circuits, the method yields efficient solutions involving a relatively small number of wavelets and simple matrix operations.

1. INTRODUCTION

When describing waveforms arising from power electronics circuits, a frequently encountered problem is the fast variations near the switching instants [1]. This usually appears as waveform ringings during the switching transitions and is caused by the presence of high-frequency resonant loops formed by small parasitic capacitances and inductances. Thus, the resulting waveforms contain largely low-frequency components with high-frequency details concentrated near the switching instants. Such a feature is consistent with the localization property of wavelets which are known in the signal processing literature to be highly suitable for describing fast changing edges embedded in slowly varying backgrounds [2]. Thus, power electronics waveforms can be efficiently approximated by an appropriate set of wavelets. In this paper we examine the use of wavelets for constructing steady-state waveforms, and our aim is to show that wavelets are suitable for approximating waveforms which are characterized by localization of high-frequency details.

2. REVIEW OF CHEBYSHEV POLYNOMIALS

We consider the following polynomial function of degree n, which is defined on the close interval $[-1,+1]$:

$$T_n(x) = \cos n(\arccos x) \tag{1}$$

where n is a non-negative integer and $0 \le \arccos x \le \pi$. The sequence of polynomials $\{T_n(x)\}$ for $n = 0, \cdots, \infty$, defines the so-called *Chebyshev polynomials of the first kind* [3]. Moreover, from $\{T_n(x)\}$, we generate polynomials of degree $n-1$, $U_{n-1}(x)$, known as *Chebyshev polynomials of the second kind:*

$$U_{n-1}(x) = \frac{T_n'(x)}{n} = \frac{\sin n(\arccos x)}{\sin(\arccos x)} \tag{2}$$

for $x \in [-1,+1]$. It can be readily shown that $U_{n-1}(x)$ has $(n-1)$ zeros in $[-1,+1]$. Let these zeros be denoted by $\eta_i^{(n)}$ for $i = 1, \cdots, n-1$, i.e., $\eta_i^{(n)} = \cos(i\pi/n)$. Note that the zeros of $U_{n-1}(x)$ are actually the extrema of $T_n(x)$. In addition, we define the end points as $\eta_0^{(n)} = 1$ and $\eta_n^{(n)} = -1$.

One important property of Chebyshev polynomials is that they are orthogonal in the sense that their inner product, defined by

$$\langle T_m, T_n \rangle \overset{\text{def}}{=} \int_{-1}^{+1} \frac{T_m(x)T_n(x)}{\sqrt{1-x^2}} dx, \tag{3}$$

has the following property:

$$\langle T_m, T_n \rangle = \begin{cases} 0 & \text{if } m \ne n \\ \pi & \text{if } m = n = 0 \\ \pi/2 & \text{if } m = n \ne 0. \end{cases} \tag{4}$$

3. WAVELET CONSTRUCTION

Wavelet construction involves two basic functions, namely the scaling function and the wavelet function. For the Chebyshev-polynomial-based wavelet construction [4, 5], the scaling and wavelet functions are

$$\phi_{j,l}(x) = \frac{\omega_j(x)}{2^j(-1)^{l+1}(x - \eta_l^{(2^j)})} \epsilon_{j,l} \tag{5}$$

$$\psi_{j,l}(x) = \frac{T_{2^j}(x)}{2^j(x - \eta_{2l+1}^{(2^{j+1})})} \left(2\omega_j(x) - \omega_j(\eta_{2l+1}^{(2^{j+1})})\right) \tag{6}$$

where l is the position index ($l = 0, 1, \cdots, 2^j$ for $\phi_{j,l}$ and $l = 0, 1, \cdots, 2^j - 1$ for $\psi_{j,l}$), j is the wavelet level ($j = 0, 1, \cdots$), defined in Section 2, $\eta_{2l+1}^{(2^{j+1})}$ is the *zero* defined in Section 2, and $\omega_j(x)$ and $\epsilon_{j,l}$ are given by

$$\omega_j(x) = (1 - x^2)U_{2^j-1}(x), \tag{7}$$

$$\epsilon_{j,l} = \begin{cases} 0.5 & \text{if } l = 0 \text{ or } l = 2^j \\ 1 & \text{if } l = 1, 2, \cdots, 2^j - 1. \end{cases} \tag{8}$$

This work was supported by Hong Kong Polytechnic University under Grant A-PD68.

0-7803-7761-3/03/$17.00 ©2003 IEEE

It can be shown that the Chebyshev-polynomial-based scaling and wavelet functions can be expressed alternatively as

$$\phi_{j,l}(x) = \frac{1}{2^{j-1}} \sum_{r=0}^{2^j} T_r(x) T_r(\eta_l^{(2^j)}) \epsilon_{j,r} \epsilon_{j,l} \quad (9)$$

$$\psi_{j,l}(x) = \frac{1}{2^{j-1}} \sum_{r=2^j+1}^{2^{j+1}} T_r(x) T_r(\eta_{2l+1}^{(2^{j+1})}) \epsilon_{j+1,r} \quad (10)$$

Obviously, the position index l runs from 0 to 2^j. Thus, there are $2^j + 1$ scaling functions and 2^j wavelet functions for a given wavelet level j. Let V_j and W_j be the space of scaling functions and that of wavelet functions, i.e.,

$$V_j = \text{span}\{\phi_{j,l} : l = 0, 1, \cdots, 2^j\} \quad (11)$$

$$W_j = \text{span}\{\psi_{j,l} : l = 0, 1, \cdots, 2^j - 1\} \quad (12)$$

Due to orthogonality, we have $\dim(V_j) = 2^j + 1$, $\dim(W_j) = 2^j$, and $V_{j+1} = V_j \oplus W_j$. Thus, for any $l = 0, 1, \cdots, 2^j$ and $k = 0, 1, \cdots, 2^j - 1$, we get

$$\langle \phi_{j,l}, \psi_{j,k} \rangle = 0. \quad (13)$$

Now, defining W_{-1} as V_0, we conclude that $W_{-1} \oplus W_0 \oplus W_1 \oplus \cdots \oplus W_j$ is a basis of $\boldsymbol{P}_{2^{j+1}}$. Thus, a combination of polynomial wavelets W_k, with $k = -1, 0, \cdots, n$, can be used to represent any polynomial function of degree 2^{j+1}.

Also, the interpolatory property gives

$$\phi_{j,l}(\eta_k^{(2^j)}) = \delta_{k,l}, \quad \psi_{j,l}(\eta_{2k+1}^{(2^{j+1})}) = \delta_{k,l} \quad (14)$$

where $\delta_{k,l}$ is the Kronecker delta function, i.e., $\delta_{k,l}$ equals 1 if $k = l$, and 0 otherwise. Clearly, the scaling and wavelet functions assume the maximum value 1 at $\eta_k^{(2^j)}$ and $\eta_{2k+1}^{(2^{j+1})}$ respectively. These points are called *interpolation points.*

4. EXPRESSING TIME DERIVATIVES OF WAVELETS — KEY TO SOLVING DIFFERENTIAL EQUATIONS

In order to use wavelets for solving differential equations, we need to map the differential operators to the wavelet basis [6]. For this purpose, polynomial wavelets are convenient [4]. Now consider the first derivative of the Chebyshev polynomial:

$$\frac{dT_n}{dx} = \begin{cases} T_0 & \text{for } n = 1 \\ 2n \sum_{m=0}^{n/2-1} T_{2m+1} & \text{for } n \geq 2 \text{ and } n \text{ even} \\ nT_0 + 2n \sum_{m=0}^{(n-1)/2} T_{2m} & \text{for } n \geq 3 \text{ and } n \text{ odd} \end{cases} \quad (15)$$

In matrix form, the above relation is $\dot{\boldsymbol{T}}_n = \overline{\boldsymbol{D}}^{(n)} \boldsymbol{T}^{(n)}$, where $\overline{\boldsymbol{D}}^{(n)}$ is an $(n+1) \times (n+1)$ matrix and $\boldsymbol{T}^{(n)}$ is the vector of Chebychev polynomials given by $\boldsymbol{T}^{(n)} = [T_0 \ T_1 \cdots T_n]^T$. Define $\boldsymbol{\Psi}^{(n)}$ as the basis of wavelets, as shown in (16) which appears on the top of next page.

Note that $\boldsymbol{\Psi}^{(n)}$ is a $(2^{n+1}+1)$-dim vector and is given by $\boldsymbol{\Psi}^{(n)} = \boldsymbol{C}^{(n)} \boldsymbol{T}^{(2^{n+1})}$, where $\boldsymbol{C}^{(n)}$ is a square matrix of size $(2^{n+1}+1)$. Here, all elements in $\boldsymbol{C}^{(n)}$ are readily found from (9) and (10). Let us now define a transform matrix: $\boldsymbol{D}^{(n)} = \boldsymbol{C}^{(n)} \overline{\boldsymbol{D}}^{(n)} \left(\boldsymbol{C}^{(n)}\right)^{-1}$. Obviously, this matrix maps the wavelets to their derivatives, i.e.,

$$\dot{\boldsymbol{\Psi}}^{(n)} = \boldsymbol{D}^{(n)} \boldsymbol{\Psi}^{(n)}. \quad (17)$$

5. STEADY-STATE SOLUTIONS OF POWER ELECTRONICS CIRCUITS

5.1. Basic Approach

Most power electronics circuits are composed of linear circuits that switch periodically among two or more circuit topologies. We may therefore describe power electronics circuits as

$$\dot{\boldsymbol{x}} = \boldsymbol{A}\boldsymbol{x} + \boldsymbol{U}(t) \quad (18)$$

where $\boldsymbol{x}$ is the m-dim state vector, $\boldsymbol{A}$ is an $m \times m$ time-varying matrix, and $\boldsymbol{U}$ is the input function. Specifically we write

$$\boldsymbol{A}(t) = \begin{bmatrix} a_{11}(t) & a_{12}(t) & \cdots & a_{1m}(t) \\ \vdots & \vdots & \ddots & \vdots \\ a_{m1}(t) & a_{m2}(t) & \cdots & a_{mm}(t) \end{bmatrix} \quad (19)$$

$$\text{and} \quad \boldsymbol{U}(t) = [u_1(t) \cdots u_m(t)]^T. \quad (20)$$

In the steady state, the solution satisfies $x(t) = x(t+T)$ for $0 \leq t \leq T$, where T is the period. Thus, we need only to approximate the solution in the closed interval $[0, T]$. Mapping the closed interval to $[-1, 1]$ by appropriate translation and scaling, we can write the boundary condition as

$$\boldsymbol{x}(+1) = \boldsymbol{x}(-1) \quad (21)$$

The basic problem now is to find the steady-state solution of (18) subject to the boundary condition (21). Specifically, we wish to approximate the solution by a weighted sum of some wavelets in $\boldsymbol{\Psi}^{(n)}$, i.e., wavelets of level n or less.

For brevity, we will omit the superscripts wherever the meanings are unambiguous. The basic approximation equation is

$$x_i(t) = \boldsymbol{K}_i^T \boldsymbol{\Psi}(t), \ \text{for} \ -1 \leq t \leq 1 \text{ and } i = 1, 2, \cdots, m \quad (22)$$

where $\boldsymbol{K}_i^T = [k_{i,0} \cdots k_{i,2^{n+1}}]$ is a coefficient vector of dimension 2^{n+1}, which is to be found. Putting (17) and (21) in (18) gives

$$\boldsymbol{K}\boldsymbol{D}\boldsymbol{\Psi} = \boldsymbol{A}(t)\boldsymbol{K}\boldsymbol{\Psi} + \boldsymbol{U}(t) \quad (23)$$

where

$$\boldsymbol{K} = \begin{bmatrix} k_{1,0} & k_{1,1} & \cdots & k_{1,2^{n+1}} \\ k_{2,0} & k_{2,1} & \cdots & k_{2,2^{n+1}} \\ \vdots & \vdots & \ddots & \vdots \\ k_{m,0} & k_{m,1} & \cdots & k_{m,2^{n+1}} \end{bmatrix}. \quad (24)$$

Thus, (22) can be written generally as

$$\boldsymbol{F}(t)\overline{\boldsymbol{K}} = -\boldsymbol{U}(t) \quad (25)$$

where $\boldsymbol{F}(t)$ is a $m \times (2^{n+1}+1)m$ matrix given by (26) shown on the top of next page, and $\overline{\boldsymbol{K}}$ is a $(2^{n+1}+1)m$-dim vector given by $\overline{\boldsymbol{K}} = \left[\boldsymbol{K}_1^T \cdots \boldsymbol{K}_m^T\right]^T$.

Note that since the unknown $\overline{\boldsymbol{K}}$ is of dimension $(2^{n+1}+1)m$, we need $(2^{n+1}+1)m$ equations. Now, the boundary condition

$$\Psi^{(n)} = \Bigg[\phi_{0,0}\ \phi_{0,1}\ \underbrace{\psi_{0,0}\ \psi_{1,0}\ \psi_{1,1}\ \psi_{2,0}\ \psi_{2,1}\ \psi_{2,2}\ \psi_{2,3}\ \cdots\ \underbrace{\psi_{k,0}\ \cdots\ \psi_{k,2^k-1}}_{2^k \text{ elements}}\ \cdots\ \psi_{n,2^n-1}}_{2^{n+1}-1 \text{ elements}}\Bigg]^T \tag{16}$$

$$F(t) = \begin{bmatrix} a_{11}(t)\Psi^T(t) - \Psi^T(t)D^T & \cdots & a_{1i}(t)\Psi^T(t) & \cdots & a_{1m}\Psi^T(t) \\ \vdots & \ddots & \vdots & \ddots & \vdots \\ a_{i1}(t)\Psi^T(t) & \cdots & a_{ii}(t)\Psi^T(t) - \Psi^T(t)D^T & \cdots & a_{im}\Psi^T(t) \\ \vdots & \ddots & \vdots & \ddots & \vdots \\ a_{m1}(t)\Psi^T(t) & \cdots & a_{mi}(t)\Psi^T(t) & \cdots & a_{mm}\Psi^T(t) - \Psi^T(t)D^T \end{bmatrix} \tag{26}$$

(21) provides m equations, i.e., $[\Psi(1) - \Psi(-1)]^T K_i = 0$, for $i = 1, \cdots, m$. Also, we obtain $2^{n+1}m$ more equations by interpolating at 2^{n+1} distinct points in the closed interval $[-1, 1]$. Let these interpolation points be $\xi_1, \xi_2, \cdots, \xi_{2^{n+1}}$. Then, the approximation equation can be written as

$$\tilde{F}\overline{K} = \tilde{U} \tag{27}$$

where

$$\tilde{F} = \begin{bmatrix} \tilde{F}_1 \\ \tilde{F}_2 \end{bmatrix} \text{ and } \tilde{U} = \begin{bmatrix} \tilde{U}_1 \\ \tilde{U}_2 \end{bmatrix} \tag{28}$$

with $\tilde{F}_1$, $\tilde{F}_2$, $\tilde{U}_1$ and $\tilde{U}_2$ given by

$$\tilde{F}_1 = \Bigg[\underbrace{\begin{matrix} [\Psi(1) - \Psi(-1)]^T & (0\ 0\ \cdots\ 0) & \cdots & (0\ 0\ \cdots\ 0) \\ (0\ 0\ \cdots\ 0) & [\Psi(1) - \Psi(-1)]^T & \cdots & (0\ 0\ \cdots\ 0) \\ \vdots & \vdots & \ddots & \vdots \\ \underbrace{(0\ 0\ \cdots\ 0)}_{2^{n+1}+1 \text{ columns}} & (0\ 0\ \cdots\ 0) & \cdots & [\Psi(1) - \Psi(-1)]^T \end{matrix}}_{(2^{n+1}+1)m \text{ columns}}\Bigg]$$

$$\tilde{F}_2 = \left.\begin{bmatrix} F(\xi_1) \\ F(\xi_2) \\ \vdots \\ \underbrace{F(\xi_{2^{n+1}})}_{(2^{n+1}+1)m \text{ columns}} \end{bmatrix}\right\} 2^{n+1}m \text{ rows} \tag{29}$$

$$\tilde{U}_1 = 0 \quad (m \text{ elements}) \tag{30}$$

$$\tilde{U}_2 = \left.\begin{bmatrix} -U(\xi_1) \\ -U(\xi_2) \\ \vdots \\ -U(\xi_{2^{n+1}}) \end{bmatrix}\right\} 2^{n+1}m \text{ elements} \tag{31}$$

By solving (27), we obtain all the coefficients necessary for generating an approximate solution for the steady-state system. One final step is to choose choice the interpolation points, ξ_k. A possible choice of the interpolation points are $\eta_i^{(2^{n+1})}$ for $i = 1, \cdots, 2^{n+1}$, which are the interpolation points of the wavelets.

5.2. Improved Approach

It should be apparent that wavelets of low levels are suited for the low-frequency part of the solution whereas those of high levels account for the high-frequency variation. Thus, by appropriately combining wavelets of different levels, solutions can be obtained more speedily.

Suppose we have selected the wavelets for approximation, say $\tilde{\Psi}_1$. Denoting the unchosen ones as $\tilde{\Psi}_2$, we partition the wavelet basis as follows.

$$\tilde{\Psi} = P\Psi = \begin{bmatrix} \tilde{\Psi}_1 \\ \tilde{\Psi}_2 \end{bmatrix} \tag{32}$$

where P is the permutation matrix defining the particular choice of wavelets. Suppose the dimension of $\tilde{\Psi}_1$ is N. Then, the dimension of $\tilde{\Psi}_2$ is $2^{n+1} + 1 - N$. The matrix $\tilde{D}$ can then be written as

$$D = PDP^{-1} = \begin{bmatrix} \tilde{D}_1 \\ \tilde{D}_2 \end{bmatrix} \tag{33}$$

where $\tilde{D}_1$ and $\tilde{D}_2$ are of size $N \times (2^{n+1} + 1)$ and $(2^{n+1} + 1 - N) \times (2^{n+1} + 1)$, respectively. Now let us retain in the solution only the part involving $\tilde{\Psi}_1$ and discard the rest, i.e., the solution is to be approximated as $K\tilde{\Psi}_1$. Then, (23) becomes

$$K_i^T \tilde{D}_1 \tilde{\Psi} = [a_{i1}(t)\ \cdots\ a_{im}(t)] \begin{bmatrix} K_1^T \\ \vdots \\ K_m^T \end{bmatrix} \tilde{\Psi}_1 + u_i(t) \tag{34}$$

for $i = 1, \cdots, m$. Thus, the size of K is $N \times m$ is substantially reduced. Comparing (34) with (25), the main difference is that the matrix $F(t)$ is much simpler. As before, the solution can be found by imposing the boundary conditions and interpolating at $N - 1$ points along the interval $[-1, 1]$. We denote these interpolation points as $\xi_1, \cdots, \xi_{N-1}$. Thus, we need to solve

$$\tilde{F}\overline{K} = \tilde{U} \tag{35}$$

where $\overline{K}$, $\tilde{F}$ and $\tilde{U}$ are as defined earlier, but are much smaller.

6. SIMULATIONS AND EVALUATIONS

In this section we apply the afore-described method to a simple flyback converter. We will evaluate the results using the *mean absolute error* (MAE) defined by MAE $= \frac{1}{2}\int_{-1}^{1} |\hat{x}(t) - x(t)|\, dt$.

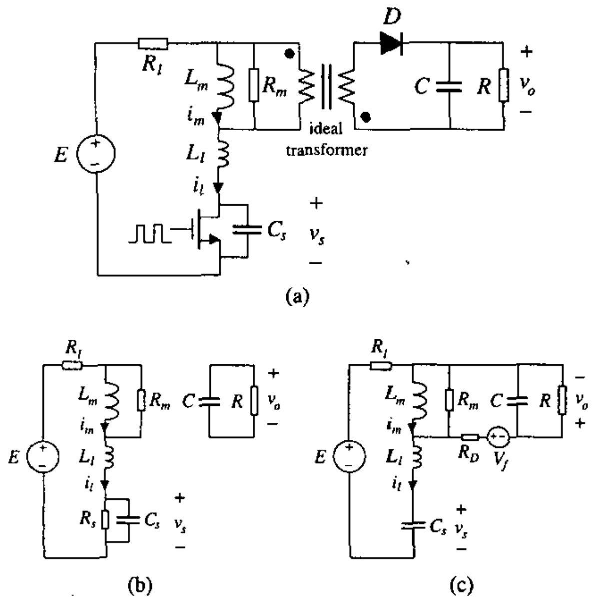

Fig. 1: (a) Flyback converter model with transformer leakage and device parasitic capacitance; (b) on-time circuit model; (c) off-time circuit model.

MAE	Number of wavelets used to approximate v_s	Number of Fourier terms used to approximate v_s
0.0500	333	516
0.0300	652	1638
0.0270	1025	1806

Table 1: Comparison of wavelet approximation and Fourier approximation for v_s in the flyback converter.

In discrete form, it is simply given by $\text{MAE} = \frac{1}{n}\sum_{i=1}^{n}|\hat{x}_i - x_i|$, where n is the total number of points sampled along the interval $[-1, 1]$ for error calculation. In the following, we use uniform sampling (i.e., equal spacing) with $n = 1001$, including boundary points.

Figure 1 (a) shows a flyback converter, where the parasitic capacitance across the switch and the leakage inductance of the transformer are deliberately included. When the switch is turned on, current flows through the magnetizing inductance L_m and the leakage inductance L_l, with the transformer secondary opened and the diode not conducting. When the switch is turned off, the transformer secondary conducts through the diode, clamping the primary voltage (i.e., voltage across L_m) to the output network (assuming a 1:1 turns ratio). Thus, L_m discharges through the transformer primary, while the leakage L_l and the parasitic capacitance C_s form a damped resonant loop around the input voltage source. Figs. 1 (b) and (c) show the detailed circuit models for the on-time and off-time. Again, the basic system equation can be readily found in the form $\dot{x} = A(t)x + U(t)$.

The main purpose of this example is to highlight the advantage gained by using wavelet approximation for waveforms containing high-frequency details around the switching instants. In order to show this, we compare the number of terms required for approximation using wavelets and conventional Fourier series. It

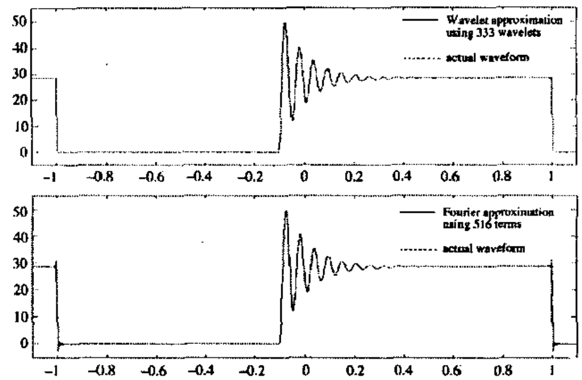

Fig. 2: Waveforms of wavelet and Fourier approximations of the switch voltage in the flyback converter.

should be noted that v_s is rich in high-frequency details due to resonant ringings. The parameters for simulation are: magnetizing (storage) inductance L_m = 0.4 mH, leakage inductance L_l= 1 μH, equivalent parallel resistance of transformer primary R_m = 1 MΩ, output capacitance C = 0.1 mF, load resistance R = 12.5 Ω, input voltage E = 16 V, diode forward drop V_f = 0.8 V, switching period T = 100 μs, on-time T_D = 45 μs, equivalent loop resistance R_l = 0.4 Ω, switch on-resistance R_S = 0.001 Ω, switch capacitance C_S = 200 nF, diode on-resistance R_D = 0.001 Ω.

In particular, we compare the number of wavelets with that of Fourier terms used to achieve the same MAE. Results are shown in Table 1. The wavelet approach is found to be advantageous as it requires fewer terms for approximation. The approximated waveforms are shown in Fig. 2.

7. CONCLUSION

A procedure has been developed for finding wavelet expansions for power electronic converters. We have shown that wavelet approximation provides an efficient means for steady-state analysis if appropriate (influential) wavelets are chosen to form the basis. Further study is necessary to establish a systematic selection procedure for forming the suitable wavelet basis for approximation.

8. REFERENCES

[1] D. Li and R. Tymerski, "A comparison of steady-state methods for power electronic circuits," *IEEE Power Electron. Spec. Conf. Rec.*, vol. 2, pp. 1084–1090, 1998.

[2] I. Daubechies, "Time-frequency localization operators: a geometric phase space approach," *IEEE Transactions on Information Theory*, vol. 34, no. 4, pp. 605–612, 1988.

[3] T.J. Rivlin, *Chebyshev Polynomials*, Second Edition, New York: Wiley Interscience, 1990.

[4] T. Kilgore and J. Prestin, "Polynomial wavelets on the interval," *Constructive Approximation*, vol. 12, pp. 95–110, 1995.

[5] G. Beylkin, "Operator in base of compactly supported wavelets," *Proc. Symp. Applied Math.*, vol. 47, 1993.

[6] S. Barmada and M. Raugi, "A general tool for circuit analysis based on wavelet transform," *Int. J. Circ. Theory Appl.*, vol. 28, pp. 461–480, 2000.